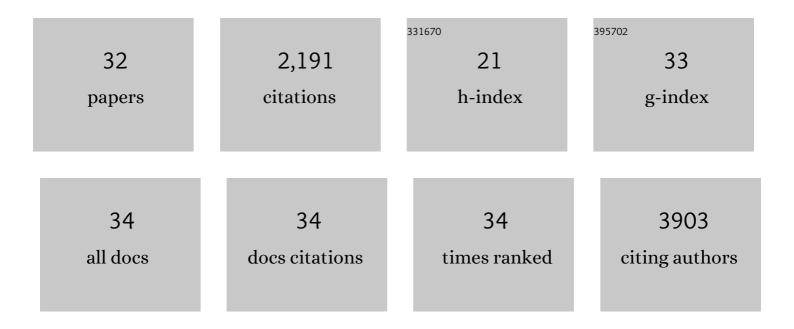
## Wojciech G Lesniak

List of Publications by Year in descending order

Source: https://exaly.com/author-pdf/7532336/publications.pdf Version: 2024-02-01



#	Article	IF	CITATIONS
1	Chemogenetics revealed: DREADD occupancy and activation via converted clozapine. Science, 2017, 357, 503-507.	12.6	813
2	A humanized antibody for imaging immune checkpoint ligand PD-L1 expression in tumors. Oncotarget, 2016, 7, 10215-10227.	1.8	158
3	PET imaging of microglia by targeting macrophage colony-stimulating factor 1 receptor (CSF1R). Proceedings of the National Academy of Sciences of the United States of America, 2019, 116, 1686-1691.	7.1	140
4	Rapid PD-L1 detection in tumors with PET using a highly specific peptide. Biochemical and Biophysical Research Communications, 2017, 483, 258-263.	2.1	132
5	PD-L1 Detection in Tumors Using [ <sup>64</sup> Cu]Atezolizumab with PET. Bioconjugate Chemistry, 2016, 27, 2103-2110.	3.6	128
6	Biodistribution of Fluorescently Labeled PAMAM Dendrimers in Neonatal Rabbits: Effect of Neuroinflammation. Molecular Pharmaceutics, 2013, 10, 4560-4571.	4.6	101
7	Peptide-based PET quantifies target engagement of PD-L1 therapeutics. Journal of Clinical Investigation, 2019, 129, 616-630.	8.2	94
8	Development of [ <sup>18</sup> F]FPy-WL12 as a PD-L1 Specific PET Imaging Peptide. Molecular Imaging, 2019, 18, 153601211985218.	1.4	52
9	Concurrent quantification of tryptophan and its major metabolites. Analytical Biochemistry, 2013, 443, 222-231.	2.4	51
10	A Distinct Advantage to Intraarterial Delivery of <sup>89</sup> Zr-Bevacizumab in PET Imaging of Mice With and Without Osmotic Opening of the Blood–Brain Barrier. Journal of Nuclear Medicine, 2019, 60, 617-622.	5.0	49
11	Noninvasive Imaging of Immune Checkpoint Ligand PD-L1 in Tumors and Metastases for Guiding Immunotherapy. Molecular Imaging, 2017, 16, 153601211771845.	1.4	47
12	Imaging glial activation in patients with post-treatment Lyme disease symptoms: a pilot study using [11C]DPA-713 PET. Journal of Neuroinflammation, 2018, 15, 346.	7.2	46
13	Optimization of osmotic blood-brain barrier opening to enable intravital microscopy studies on drug delivery in mouse cortex. Journal of Controlled Release, 2020, 317, 312-321.	9.9	35
14	PET imaging of distinct brain uptake of a nanobody and similarly-sized PAMAM dendrimers after intra-arterial administration. European Journal of Nuclear Medicine and Molecular Imaging, 2019, 46, 1940-1951.	6.4	33
15	A fully human CXCR4 antibody demonstrates diagnostic utility and therapeutic efficacy in solid tumor xenografts. Oncotarget, 2016, 7, 12344-12358.	1.8	32
16	Fetal uptake of intra-amniotically delivered dendrimers in a mouse model of intrauterine inflammation and preterm birth. Nanomedicine: Nanotechnology, Biology, and Medicine, 2014, 10, 1343-1351.	3.3	30
17	Evaluation of PSMA-Targeted PAMAM Dendrimer Nanoparticles in a Murine Model of Prostate Cancer. Molecular Pharmaceutics, 2019, 16, 2590-2604.	4.6	29
18	The distribution of the alpha7 nicotinic acetylcholine receptor in healthy aging: An in vivo positron emission tomography study with [18F]ASEM. NeuroImage, 2018, 165, 118-124.	4.2	27

WOJCIECH G LESNIAK

#	Article	IF	CITATIONS
19	Hyperosmolar blood–brain barrier opening using intra-arterial injection of hyperosmotic mannitol in mice under real-time MRI guidance. Nature Protocols, 2022, 17, 76-94.	12.0	26
20	Bridged cyclams as imaging agents for chemokine receptor 4 (CXCR4). Nuclear Medicine and Biology, 2014, 41, 552-561.	0.6	25
21	In vivo Evaluation of an Engineered Cyclotide as Specific CXCR4 Imaging Reagent. Chemistry - A European Journal, 2017, 23, 14469-14475.	3.3	25
22	High Availability of the α7-Nicotinic Acetylcholine Receptor in Brains of Individuals with Mild Cognitive Impairment: A Pilot Study Using <sup>18</sup> F-ASEM PET. Journal of Nuclear Medicine, 2020, 61, 423-426.	5.0	22
23	Dual contrast agents for fluorescence and photoacoustic imaging: evaluation in a murine model of prostate cancer. Nanoscale, 2021, 13, 9217-9228.	5.6	19
24	<sup>18</sup> F-XTRA PET for Enhanced Imaging of the Extrathalamic α4β2 Nicotinic Acetylcholine Receptor. Journal of Nuclear Medicine, 2018, 59, 1603-1608.	5.0	15
25	Structural Characterization and in Vivo Evaluation of β-Hairpin Peptidomimetics as Specific CXCR4 Imaging Agents. Molecular Pharmaceutics, 2015, 12, 941-953.	4.6	13
26	<sup>11</sup> C-PABA as a PET Radiotracer for Functional Renal Imaging: Preclinical and First-in-Human Study. Journal of Nuclear Medicine, 2020, 61, 1665-1671.	5.0	11
27	PET imaging of soluble epoxide hydrolase in non-human primate brain with [18F]FNDP. EJNMMI Research, 2020, 10, 67.	2.5	10
28	Dual-Modality PET–SPECT Image-Guided Pretargeting Delivery in HER2(+) Breast Cancer Models. Biomacromolecules, 2021, 22, 4606-4617.	5.4	7
29	First-in-human neuroimaging of soluble epoxide hydrolase using [18F]FNDP PET. European Journal of Nuclear Medicine and Molecular Imaging, 2021, 48, 3122-3128.	6.4	6
30	An Evaluation of CXCR4 Targeting with PAMAM Dendrimer Conjugates for Oncologic Applications. Pharmaceutics, 2022, 14, 655.	4.5	4
31	A side-by-side evaluation of [18F]FDOPA enantiomers for non-invasive detection of neuroendocrine tumors by positron emission tomography. Oncotarget, 2019, 10, 5731-5744.	1.8	3
32	Measurement of PET Quantitative Bias In Vivo. Journal of Nuclear Medicine, 2021, 62, 732-737.	5.0	3